Medicine®

SYSTEMATIC REVIEW AND META-ANALYSIS

OPEN

Gadolinium Ethoxybenzyl Diethylenetriamine Pentaacetic Acid (Gd-EOB-DTPA)-Enhanced Magnetic Resonance Imaging and Multidetector-Row Computed Tomography for the Diagnosis of Hepatocellular Carcinoma

A Systematic Review and Meta-analysis

Feng Ye, MD, Jun Liu, and Han Ouyang, MD

Abstract: The purpose of this meta-analysis was to compare the diagnostic accuracy of gadolinium ethoxybenzyl diethylenetriamine pentaacetic acid (Gd-EOB-DTPA)-enhanced magnetic resonance imaging (MRI) and multidetector-row computed tomography (MDCT) for hepatocellular carcinoma (HCC).

Medline, Cochrane, EMBASE, and Google Scholar databases were searched until July 4, 2014, using combinations of the following terms: gadoxetic acid disodium, Gd-EOB-DTPA, multidetector CT, contrast-enhanced computed tomography, and magnetic resonance imaging. Inclusion criteria were as follows: confirmed diagnosis of primary HCC by histopathological examination of a biopsy specimen; comparative study of MRI using Gd-EOB-DTPA and MDCT for diagnosis of HCC; and studies that provided quantitative outcome data. The pooled sensitivity and specificity of the 2 methods were compared, and diagnostic accuracy was assessed with alternative-free response receiver-operating characteristic analysis.

Nine studies were included in the meta-analysis, and a total of 1439 lesions were examined. The pooled sensitivity and specificity for 1.5T MRI were 0.95 and 0.96, respectively, for 3.0T MRI were 0.91 and 0.96, respectively, and for MDCT were 0.74 and 0.93, respectively. The pooled diagnostic odds ratio for 1.5T and 3.0T MRI was 242.96, respectively, and that of MDCT was 33.47. To summarize, Gd-EOB-DTPA-enhanced MRI (1.5T and 3.0T) has better diagnostic accuracy for HCC than MDCT.

(*Medicine* 94(32):e1157)

Abbreviations: AUC = area under curve, FN = false negative, FP = false positive, Gd-EOB-DTPA = gadolinium ethoxybenzyl diethylenetriamine pentaacetic acid, HCC = hepatocellular carcinoma, MDCT = multidetector-row computed tomography, MRI = magnetic resonance imaging, QUADAS = quality assessment of diagnostic studies, SE = standard error, SROC = summary receiver-operating characteristic, TN = true negative, TP = true positive.

INTRODUCTION

Hepatocellular carcinoma (HCC) is the fifth most common cancer, and the third most common cause of cancer deaths worldwide.[1] Early detection and accurate assessment of HCC are therefore very important, as early stages of HCC are potentially curable,[2] with diagnostic imaging playing a major role in the detection, characterization, staging, and treatment monitoring of patients with HCC or liver metastases.

Computed tomography (CT) and magnetic resonance imaging (MRI) are both commonly used imaging modalities for diagnosis and evaluation of liver lesions.[2–4] Compared with regular single-detector CT, multidetector-row computed tomography (MDCT) has advantages of providing greater speed, thinner slices, and multiphasic scanning, which improve spatial and temporal resolution, and provide a more precise evaluation of liver tumor's hemodynamics thereby improving the overall diagnostic accuracy.[3] On the contrary, dynamic MRI using a fast 3-dimensional T1-weighted gradient echoimaging sequence with a nonspecific contrast medium can also be highly sensitive in detecting hypervascular HCC.[3,4]

Gadolinium ethoxybenzyl diethylenetriamine pentaacetic acid (Gd-EOB-DTPA; gadoxetic acid disodium; Primovist, Bayer Schering Pharma, Berlin, Germany) is a liver-specific contract agent for MRI imaging.[5] Approximately 50% of injected GD-EOB-DTPA is taken up by functioning hepatocytes and excreted in the bile, thus enabling hepatobiliary phase imaging to begin approximately 10 to 20 minutes after injection.[4,5] Studies have shown that GD-EOB-DTPA MRI provides excellent diagnostic accuracy for both HCC[6] and incidental lesions in the liver.[7] Some even suggested that GD-EOB-DTPA-enhanced MRI may replace CT arterial portography (CTAP) and CT hepatic arteriography (CTHA).[6]

Although a number of studies have suggested that GD-EOB-DTPA-enhanced MRI provides a better diagnostic performance than MDCT for HCC,[8–12] there has been no in-depth meta-analysis performed to compare the 2 methods with respect to their diagnostic accuracies. Thus, the purpose of this study was to perform a meta-analysis comparing the diagnostic accuracy of GD-EOB-DTPA-enhanced MRI and MDCT for the diagnosis of HCC.

Editor: Wenyu Lin.
Received: January 28, 2015; revised: June 5, 2015; accepted: June 23, 2015.
From the Department of Radiology (FY, HO), Cancer Hospital Chinese Academy of Medical Science, Beijing; and Department of Radiology (JL), The 5th People's Hospital of Shanghai, Shanghai, China.
Correspondence: Han Ouyang, Department of Radiology, Cancer Hospital Chinese Academy of Medical Science, No. 17 Panjiayuannanli, Chaoyang District, Beijing 100021, China (e-mail: ouyangh666@sina.com).
The authors have no funding and conflicts of interest to disclose.

ISSN: 0025-7974
DOI: 10.1097/MD.0000000000001157

MATERIALS AND METHODS

Ethic Statement

Meta-analyses do not involve human subjects and do not require Institutional Review Board review (*J Grad Med Educ*. 2011 March; 3(1): 5–6.).

Literature Search Strategy

This systematic review and meta-analysis was performed in accordance with the PRISMA guidelines.[13] We have searched various databases including Medline, Cochrane, EMBASE, and Google Scholar until July 4, 2014, using the following terms or their combinations: gadoxetic acid disodium, Gd-EOB-DTPA, multidetector CT, contrast-enhanced computed tomography, and magnetic resonance imaging. The inclusion criteria of our study were as follows: confirmed diagnosis of primary HCC by histopathological examination of a biopsy or resected specimen; comparative study of MRI using Gd-EOB-DTPA as the contrast agent and MDCT for diagnosis of HCC; and studies that provided quantitative data for the outcomes. Non-English publications, letters, comments, editorials, case reports, proceedings, and personal communications were excluded. We also excluded studies that did not provide sufficient data for the outcomes to be analyzed. Reference lists of relevant studies or reviews were also manually searched for additional records that might qualify for inclusion.

The quality assessment of diagnostic studies (QUADAS) tool[14] was used by 2 independent reviewers to assess diagnostic accuracy and rate the quality of each study included in this meta-analysis.

Data Extraction

Studies were identified via the search strategy by 2 independent reviewers, and a third reviewer was consulted when disagreement arose. Data extracted from studies that met the inclusion criteria include name of the first author, year of publication, study design, number of patients in each imaging group and their age and sex, locations and stages of tumors, and the numbers of lesions that were true positive (TP), false positive (FP), true negative (TN), and false negative (FN) for each imaging modality.

Outcome Measures and Data Analysis

The primary outcomes were the sensitivity and specificity of GD-EOB-DTPA-enhanced MRI and MDCT for the diagnosis of primary HCC. The sensitivity and specificity with corresponding 95% confidence intervals (95% CIs) were calculated and presented by a forest plot. A χ^2-based test of homogeneity was performed using Cochran Q test and I^2 statistics.[15] I^2 statistic indicates the percentage of the total variability in the effect estimates among trials due to heterogeneity rather than chance. Random-effects models of analysis were used if heterogeneity was detected (Cochran Q test $P < 0.1$ or $I^2 > 50\%$), and the pooled sensitivity and specificity were derived using the DerSimonian–Laird method. Otherwise, fixed-effects models were used and the pooled sensitivity and specificity were derived using the Mantel–Haenszel method instead.

Summary receiver-operating characteristic (SROC) curves for MRI and MDCT were constructed using the false-positive rate (FPR = 1-specificity) and true positive rate (TPR = sensisensitivity). The area under the SROC curve (AUC) with standard error (SE) was estimated for the diagnostic accuracy of each imaging method. An AUC that is >0.5 and closer to 1.0 implies better accuracy.[15] Moreover, a diagnostic odds ratio (DOR) and index Q^* value with SE were calculated for the discriminating ability of the imaging methods. A higher DOR value indicates better discriminatory performance for a diagnostic test. Both the DOR and the Q^* values were used to compare the diagnostic performance of MRI and MDCT based on the z-statistic test.[16] In addition, the Moses model was used to examine the symmetry of data according to the coefficient b of the model,[16] and the results were reported as either asymmetric or symmetric. A coefficient $b = 0$ would indicate the SROC curve's being symmetric. All the statistical analyses were performed using MetaDiSc version 1.4 (Clinical Biostatistics Unit, Ramón y Cajal Hospital, Madrid, Spain).

RESULTS

Literature Search

A flow diagram of the study selection is shown in Figure 1A. A total of 178 articles were identified in the initial search, and after removal of duplicates, 55 articles remained. Of these 55 articles, 32 were excluded based on the inclusion and exclusion criteria. Fourteen of the remaining 23 articles were excluded for either not providing data for the outcome of interest (n = 6) or not providing sufficient data for calculation with respect to the outcome of interest (n = 8). Thus, 9 studies were included in the meta-analysis.[8–12,17–20] The results of the QUADAS used to assess the quality of each study are shown in Figure 1B.

Study Characteristics

The 9 studies included a total of 469 patients (Table 1). The number of patients in the studies ranged from 29 to 75, and the mean patient ages were similar among the studies and ranged from 54.7 to 68.8 years. The percentages of males were >50% in all the studies (range, 55%–87%), and a total of 1439 lesions were examined. Six studies used 1.5T MRI[8,10–12,17,18] and 3 studies used 3.0T MRI.[9,19,20] The diagnostic results (numbers of TP, TN, FP, and FN lesions) of the imaging systems used in the studies are summarized in Table 2.

Forest plots of sensitivity, specificity, and SROC curves for the diagnostic accuracy of 1.5T MRI are shown in Figure 2A–C, respectively. I^2 and Cochran Q tests indicated the presence of heterogeneity among studies in sensitivity, but not in specificity (sensitivity: $I^2 = 69.5\%$, Cochran Q test $P = 0.0058$; specificity: $I^2 = 0\%$, Cochran Q test $P = 0.9289$). The pooled sensitivity and specificity were 0.95 (95% CI: 0.88 to 0.93) and 0.96 (95% CI: 0.94 to 0.97), respectively. The SROC curve was symmetric, and the AUC = 0.987 (SE = 0.004). These results indicate that 1.5T MRI exhibits excellent diagnostic accuracy with respect to HCC.

Forest plots of sensitivity, specificity, and SROC curve for the diagnostic accuracy of 3.0T MRI are shown in Figure 3A–C, respectively. I^2 and Cochran Q tests indicated the presence of heterogeneity among studies in sensitivity, but not in specificity (sensitivity: $I^2 = 69.5\%$, Cochran Q test $P = 0.0058$; specificity: $I^2 = 0\%$, Cochran Q test $P = 0.9289$). The pooled sensitivity and specificity were 0.91 (95% CI: 0.88 to 0.93) and 0.96 (95% CI: 0.94 to 0.97), respectively. The SROC curve was symmetric, and the AUC = 0.987 (SE = 0.004). These results indicate that 3.0T MRI exhibits excellent diagnostic performance with respect to HCC. Furthermore, nearly identical index Q^* values and SE of 1.5T and 3.0T MRI (Figures 2C and 3C) indicate that MRI of both strengths provide very similar and excellent diagnostic performance.

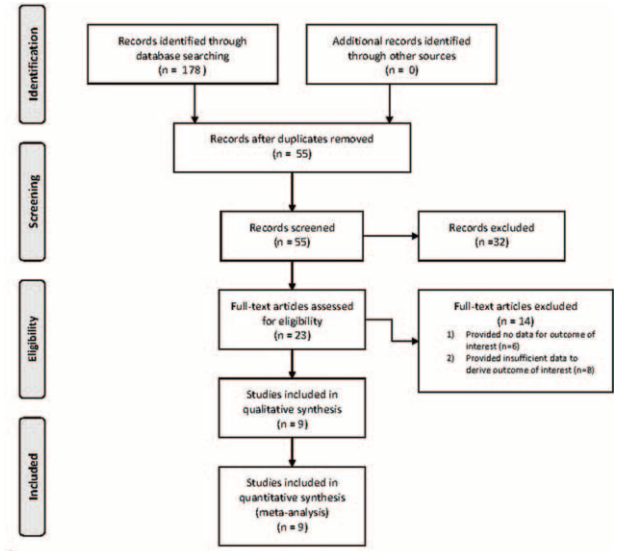

A

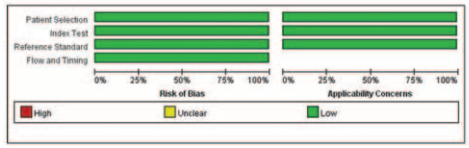

B

FIGURE 1. (A) Flow diagram of study selection, and (B) quality assessment of included articles using quality assessment of diagnostic studies (QUADAS) tool.

Forest plots of sensitivity, specificity, and SROC curve for the diagnostic performance of MDCT are shown in Figure 4A–C, respectively. I^2 and Cochran Q tests indicated the presence of heterogeneity in both sensitivity and specificity among the studies (sensitivity: $I^2 = 81.5\%$, Cochran Q test $P < 0.001$; specificity: $I^2 = 83.6\%$, Cochran Q test $P < 0.001$). The pooled sensitivity and specificity were 0.74 (95% CI: 0.70 to 0.77) and 0.93 (95% CI: 0.91 to 0.94), respectively. The SROC curve was symmetric, and the AUC = 0.884 (SE = 0.053). These results indicate that MDCT provides good diagnostic performance.

The DORs of 1.5T MRI, 3.0T MRI, and MDCT are shown in Figure 5A–C, respectively. I^2 and Cochran Q tests indicated the presence of heterogeneity in the MDCT imaging system only (MRI 1.5T or 3.0T: $I^2 = 35.3\%$, Cochran Q test $P = 0.1720$; MDCT: $I^2 = 85.6\%$, Cochran Q test $P < 0.001$). The pooled DORs for both 1.5T and 3.0T MRI were 242.96 (95% CI: 114.99 to 513.32, Figure 5A and B), and the pooled DOR for MDCT was 33.47 (95% CI 12.48 to 89.79, Figure 5C).

The index Q^* values were 0.812 (SE = 0.0549) and 0.9526 (SE = 0.0089) for MDCT and MRI, respectively (both 1.5T and 3.0T had the same index Q^* values). The index Q^* value of MRI's being closer to 1 than that of MDCT indicate that MRI is superior to MDCT in diagnostic accuracy of HCC. The z-test also showed the SROC curves of MRI and MDCT to be significantly different ($z = 2.47$, $P = 0.0072$).

DISCUSSION

This meta-analysis comparing Gd-EOB-DTPA-enhanced MRI and MDCT for the diagnosis of HCC showed that while MDCT provided good diagnostic performance, both 1.5T and 3.0T MRI provided superior diagnostic accuracy than MDCT.

For many years, CT has been the primary imaging method for evaluating the liver lesions, and the diagnostic accuracy has improved with recent advance in technology such as MDCT.[3] When MRI was first introduced, its ability for evaluating lesions in the liver was not as good as CT, but with advances such as gradient echoimaging and new contract agents, MRI has become highly sensitive for evaluating liver lesions, in particular, for the detection of hypervascular HCC.[3,4] Gd-EOB-DTPA has high T1 relaxivity in the liver, and enhancement occurs on early perfusion and delayed hepatobiliary phase images.[21] Immediately after injection, Gd-EOB-DTPA distributes in the extracellular fluid space, and its uptake into hepatic cells begins 1 to 2 minutes later, followed by excretion via bile and the kidneys.[21] The enhanced hepatic signal intensity peaks about 20 minutes after injection.[21] The introduction of Gd-EOB-DTPA has further increased the ability of MRI to diagnose liver lesions, and studies have shown the diagnostic performance of Gd-EOB-DTPA-enhanced MRI to rival[22,23] or even surpass that of MDCT.[24–28]

Hwang et al[29] studied 54 patients with chronic liver disease with 59 HCCs $\leq$ 2 cm in diameter, and reported that Gd-EOB-DTPA MRI exhibited better diagnostic performance than 64-MDCT. Similarly, Inoue et al[30] reported that the diagnostic ability of Gd-EOB-DTPA-enhanced MRI for both hypovascular tumors and hypervascular HCCs <2 cm was superior to that of dynamic MDCT. In a multicenter study that included 178 patients with focal hepatic lesions, Ichikawa et al[31] found that Gd-EOB-DTPA-enhanced MRI provided better detection and characterization of the lesions compared to triphasic contrast-enhanced spiral CT, most specifically for smaller lesions and in cases of liver cirrhosis. It has also been suggested that Gd-EOB-DTPA-enhanced MRI may provide better accuracy for treatment decisions in patients with early-stage HCC than MDCT.[32] With respect to metastatic disease, a study of colorectal tumor liver metastases by Zech et al[33] reported that the diagnostic performance of Gd-EOB-DTPA-enhanced MRI was superior to that of both contrast-enhanced CT and MRI using an extracellular contrast medium.

Studies have examined the diagnostic ability of Gd-EOB-DTPA-enhanced MRI for the detection of HCC[34] and liver metastases[35] without comparison to other imaging or diagnostic modalities. Liu et al[34] performed a meta-analysis that included 10 studies to examine the diagnostic accuracy of Gd-EOB-DTPA-enhanced MRI for the detection of HCC. The overall pooled weighted sensitivity, specificity, DOR, positive likelihood ratio, negative likelihood ratio, and AUC were 0.91, 0.95, 169.94, 15.75, 0.10, and 0.9778, respectively, for HCC, and 0.91, 0.93, 234.24, 15.08, 0.08, and 0.9814 for patients with

TABLE 1. Basic Characteristics of the Included Studies

First Author/Year of Publication	Number of Patients	Age, y	Male	Number of Tumors	Tumor Size, mm	MRI Field Strength	Type of CT	CT Contrast Agent
Böttcher (2013)[10]	29	64 (22, 84)	55%	130	22 ± 17	1.5T	64-MDCT	Nonionic, monomeric, iodinated contrast medium (300 mg of iodine/mL). Contrast agent (120 mL iopromide) was administered by a power injector with a flow rate of 3.5 mL/s followed by a 50-mL 0.9% saline flush with the same flow rate.
Ooka (2013)[17]	54	68.8 ± 10.5	74%	441	18.4 ± 10.8	1.5T	CTAP/CTHA was performed using an IVR-CT system (Infinix Active; Toshiba Medical Systems, Tokyo, Japan) comprised of a digital subtraction angiography system (CAS-8000 V/DFP-2000A; Toshiba Medical Systems) and a 4-detector MDCT scanner	Contrast agent was administered at a rate of 2 mL/s through the cubital vein, which was flushed with 20 mL of saline using a power injector.
Baek (2012)[9]	51	(32, 80)	84%	110	29.8 (2, 100)	3T	64-channel and 16-channel MDCT	Nonionic contrast medium at a dose of 2 mL/kg body weight.
Akai (2011)[8]	34	65 (48, 78)	79%	106	24 (6, 152)	1.5T	Triple-phase 64-MDCT	Nonionic contrast material at a dose of 2 mL/kg body weight to a maximum dose of 100 mL using a power injector at a rate of 3 mL/s.
Haradome (2011)[12]	75	54.7 (42, 67)	80%	99	17.4 ± 6.53	1.5T	16-channel MDCT	Nonionic contrast medium containing a high concentration of iodine (370 mg of iodine/kg). The volume of delivered contrast medium was determined according to patient body weight (1.8 mL/kg body weight).
Sano (2011)[18]	64	65.6 ± 9.5	73%	252	12.7 ± 5.0	1.5T	CTHA and CTAP performed with a 16-detector row scanner	20 mL of nonionic contrast medium (Omnipaque 300, Iomeron 350, Iopamiron 370) diluted with 60 mL of saline delivered via a catheter in the common hepatic artery.
Di Martino (2010)[11]	58	63 (35, 84)	67%	109	18 ± 15	1.5T	Multiphasic 64-section MDCT	Nonionic contrast medium (Iomeprol, 400 mg of iodine/mL [Iomeron 400; Bracco Imaging, Milan, Italy]) at a dose of 1.3 mL (520 mg of iodine)/kg body weight
Sun (2010)[19,*]	42	55.8 (39, 73)	81%	60	13.7 ± 4.1	3.0T	8, 16, and 64-MDCT	90–150 mL (1.5 mL/kg body weight) of nonionic contrast material (Ultravist 370 [iopromide]; Schering, Germany) through an 18-guage intravenous catheter inserted into a forearm vein using an MK-IV dedicated CT injector at a rate of 3–5 mL/s for 30 s.
Kim (2009)[20]	62	55 (31, 67)	87%	132	29 (5, 105)	3.0T	16, 40, or 64-MDCT	120 mL of a nonionic iodinated contrast agent (Iopamidol, Iopamiro 300, Bracco, Milano, Italy) at a rate of 3-4 mL/s with a bolus-triggered technique.

CT = computed tomography, CTAP = computed tomography arterial portography, CTHA = computed tomography hepatic arteriography, HCC = hepatocellular carcinoma, MDCT = multidetector computed tomography, MRI = magnetic resonance imaging. Age and tumor size were summarized as mean ± standard deviation, or as median with range: (min, max).

* In the Sun (2010)[19] study, there were total 69 patients and 44 HCCs, but only 42 patients with 60 arterial enhancing lesions received both MRI and CT. Data for age, percent males, and tumor size are reported for the 69 patients.

TABLE 2. Diagnostic Outcomes of the Included Studies

First Author/Year of Publication	MRI				CT			
	TP	FP	FN	TN	TP	FP	FN	TN
Böttcher (2013)[10]	61	2	7	60	44	16	24	46
Ooka (2013)[17]	83	15	4	339	74	11	13	343
Baek (2012)[9]	67	3	6	34	55	0	18	37
Akai (2011)[8]	46	2	6	52	40	3	12	55
Haradome (2011)[12]	47	2	13	37	43	2	17	37
Sano (2011)[18]	88	6	3	155	55	15	36	146
Di Martino (2010)[11]	79	2	8	20	61	6	26	16
Sun (2010)[19]	31	2	2	25	18	1	15	26
Kim (2009)[20]	78	1	5	45	77	6	6	43

CT = computed tomography, FN = false negative, FP = false positive, MRI = magnetic resonance imaging, TN = true negative, TP = true positive.

cirrhosis; notably, the AUC for HCC ≤2 cm was 0.9936. Chen et al[35] similarly performed a meta-analysis examining the diagnostic accuracy of Gd-EOB-DTPA-enhanced MRI for the detection of liver metastases that included 13 studies and 1900 lesions, and their reported pooled weighted sensitivity, specificity, positive and negative likelihood ratios, DOR, and AUC were 0.93, 0.95, 18.07, 0.07, 249.81, and 0.98, respectively.

The 9 studies included in our meta-analysis contain data recently published from 2009 to 2013. In the earliest included report (2009), Kim et al[20] studied 62 patients with 83 surgically proven HCCs that received initial diagnoses using either triple-phase 16, 40, or 64-MDCT, or 3.0T Gd-EOB-DTPA-enhanced MRI. Although the overall performance of the 2 imaging techniques was similar, more small tumors (<1 cm) were detected by MRI than CT even though this difference was not statistically significant due to the small sample size (only 10 of 83 HCC were <1 cm). Two included studies were performed in 2013. Böttcher et al[10] performed Gd-EOB-DTPA MRI and MDCT on 29 patients with 130 focal liver lesions and reported detection rates of 91.5% and 80.4%, respectively ($P < 0.05$); the sensitivity, specificity, and diagnostic accuracy of MRI and MDCT were 86.8%, 94.4%, and 90.4%, and 66.2%, 79.0%, and 72.3%, respectively ($P < 0.05$). In another study published in

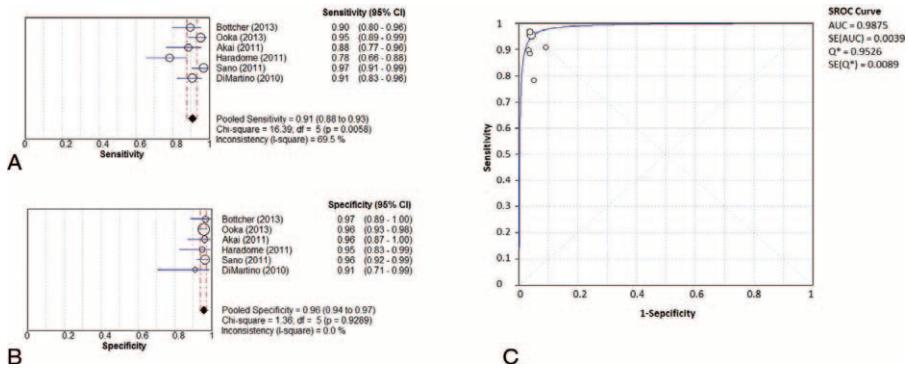

FIGURE 2. Forest plots of (A) sensitivity, (B) specificity, and (C) SROC curve for the diagnostic performance of 1.5T MRI. 95% CI = 95% confidence interval, AUC = area under SROC curve, MRI = magnetic resonance imaging, SE = standard error, SROC = summary receiver-operating characteristic.

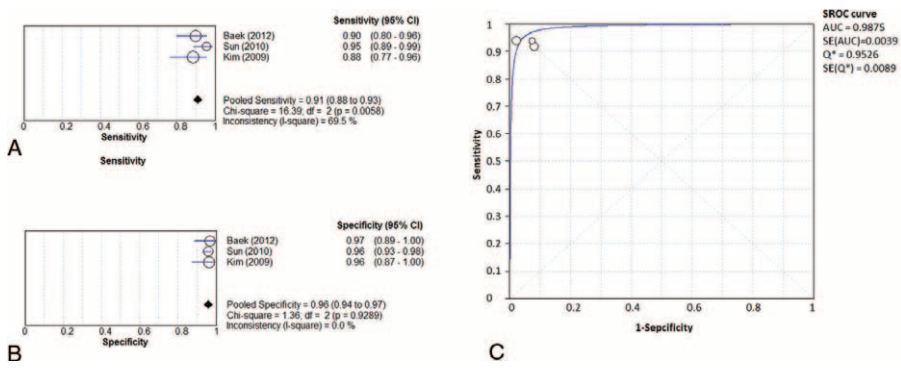

FIGURE 3. Forest plots of (A) sensitivity, (B) specificity, and (C) SROC curve for the diagnostic performance of 3.0T MRI. 95% CI = 95% confidence interval, AUC = area under SROC curve, MRI = magnetic resonance imaging, SE = standard error, SROC = summary receiver-operating characteristic.

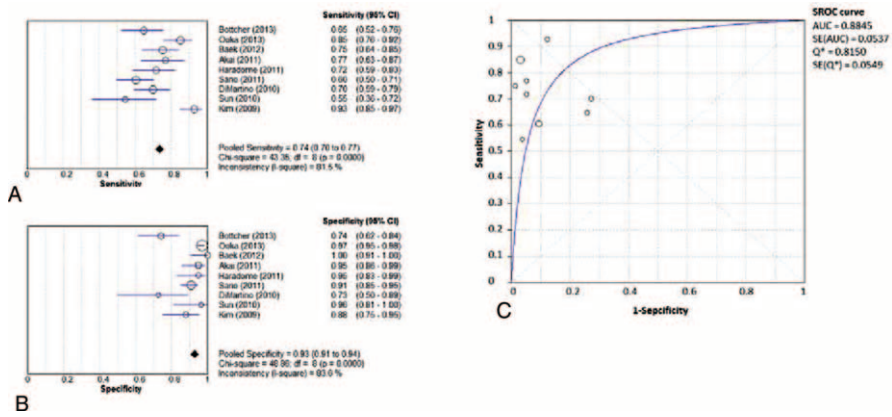

FIGURE 4. Forest plots of (A) sensitivity, (B) specificity, and (C) SROC curve for the diagnostic performance of MDCT. 95% CI = 95% confidence interval, AUC = area under SROC curve, MDCT = multidetector computed tomography, SE = standard error, SROC = summary receiver-operating characteristic.

2013, Ooka et al[17] retrospectively examined the records of 54 patients with 87 nodular HCCs evaluated with CTAP/CTHA and Gd-EOB-DTPA-enhanced MRI. Three blinded readers reviewed the radiographic data, and for all 3 readers, the mean AUC was significantly greater for MRI than CT images (0.98 vs 0.93, respectively, $P = 0.0009$). Although the sensitivity was the same for both the methods, the sensitivity for detecting lesions $\leq$20 mm was significantly higher with MRI than CT for all the 3 readers.

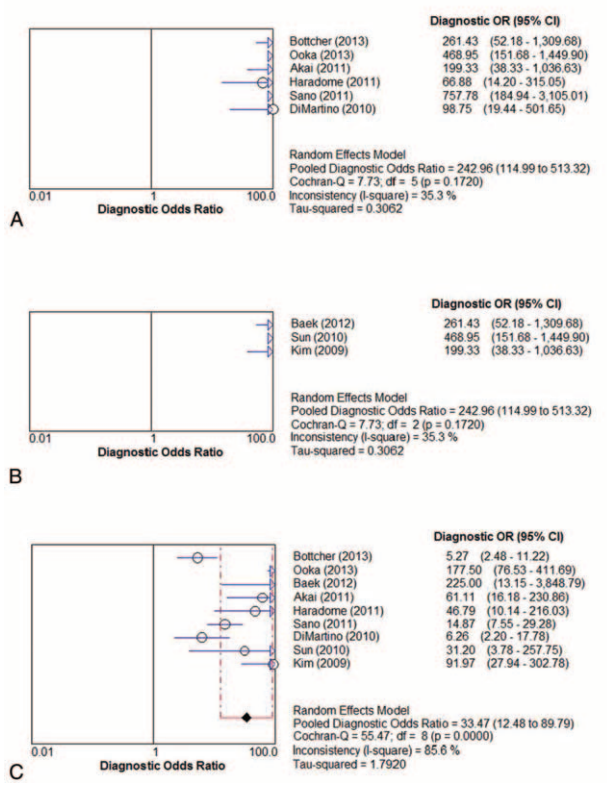

FIGURE 5. Forest plots of the diagnostic ORs with 95% CIs for the diagnostic performance of (A) 1.5T MRI, (B) 3.0T MRI, and (C) MDCT. 95% CI = 95% confidence interval, MDCT = multidetector computed tomography, MRI = magnetic resonance imaging, OR = odd ratio.

Results of this study suggest that there is no difference between the diagnostic accuracy of 1.5T and 3.0T MRI with Gd-EOB-DTPA as the contrast agent for the diagnosis of HCC. However, it should be noted that there were no controlled studies that compared the diagnostic accuracy of 1.5T and 3.0T MRI included in this analysis, and there is only a limited number of studies in literature that assess the accuracy of 1.5T and 3.0T MRI in HCC. Kim et al[36] compared 1.5T and 3.0T MRI with Gd-EOB-DTPA as the contrast agent for the detection of HCC and reported that both exhibited similar diagnostic performance for detecting small HCCs, but there was a tendency toward increased reader confidence for the arterial and hepatocyte phase with 3.0T compared with 1.5T. In a study that attempted to correlate superparamagnetic iron oxide-enhanced MRI findings of well-differentiated HCC with those of MDCT, Kim et al[37] reported that 83% of lesions examined with 1.5T MRI were hyperintense as compared with 88% of lesions examined with 3.0T MRI, but the difference was non-significant ($P = 0.745$).

There are limitations of this study that should be considered. The number of studies included in the analysis was relatively small, but a total of 1536 lesions were examined. There was heterogeneity in the imaging parameters used among included studies, and the equipment used and the operators' expertise also varied. Furthermore, MRI and MDCT imaging studies were performed only in patients who did not pass a screening test. Though this was based on the American Association for the Study of Liver Diseases guidelines,[2] it could lead to bias in patient selection. In addition, not all nodules/lesions identified on imaging studies could be resected and the diagnosis confirmed by histopathological examination. Only nodules or lesions mostly likely to be tumors were resected, so evaluation of other types of lesions was not performed. These 2 limitations may lead to a lower rate of FN lesions and an overestimation of the actual sensitivities of both imaging techniques. No distinction was made between cirrhotic and non-cirrhotic patients, and the manufacturer's suggestion of performing hepatobiliary phase imaging 20 minutes after Gd-EOB-DTPA administration might not yield optimal results for cirrhotic patients in whom contrast uptake and elimination

would be delayed. Also, we did not use tumor size as a criterion, such that we were able to include more studies in the meta-analysis. But based on the reported data of the included studies, MRI shows better diagnostic accuracy with tumors as small as 1.2 cm. Furthermore, we did not evaluate cost-effectiveness ratio in our study, but cost may drop in the future and better diagnostic accuracy can potentially save lives or improve life quality that may eventually outweigh cost consideration.

In conclusion, this meta-analysis of 9 recently published studies indicates that Gd-EOB-DTPA-enhanced MRI provides better sensitivity and specificity than MDCT for the diagnosis of primary HCC.

REFERENCES

1. Jemal A, Bray F, Center MM, et al. Global cancer statistics. *CA Cancer J Clin.* 2011;61:69–90.
2. Bruix J, Sherman M. Practice Guidelines Committee, American Association for the Study of Liver Diseases. Management of hepatocellular carcinoma. *Hepatology.* 2005;42:1208–1236.
3. O'Neill EK, Cogley JR, Miller FH. The ins and outs of liver imaging. *Clin Liver Dis.* 2015;19:99–121.
4. Lee JM, Yoon JH, Kim KW. Diagnosis of hepatocellular carcinoma: newer radiological tools. *Semin Oncol.* 2012;39:399–409.
5. Palmucci S. Focal liver lesions detection and characterization: the advantages of gadoxetic acid-enhanced liver MRI. *World J Hepatol.* 2014;6:477–485.
6. Murakami T, Okada M, Hyodo T. CT versus MR imaging of hepatocellular carcinoma: toward improved treatment decisions. *Magn Reson Med Sci.* 2012;11:75–81.
7. Chung YE, Kim MJ, Kim YE, et al. Characterization of incidental liver lesions: comparison of multidetector CT versus Gd-EOB-DTPA-enhanced MR imaging. *PLoS One.* 2013;8:e66141.
8. Akai H, Kiryu S, Matsuda I, et al. Detection of hepatocellular carcinoma by Gd-EOB-DTPA-enhanced liver MRI: comparison with triple phase 64 detector row helical CT. *Eur J Radiol.* 2011;80:310–315.
9. Baek CK, Choi JY, Kim KA, et al. Hepatocellular carcinoma in patients with chronic liver disease: a comparison of gadoxetic acid-enhanced MRI and multiphasic MDCT. *Clin Radiol.* 2012;67:148–156.
10. Böttcher J, Hansch A, Pfeil A, et al. Detection and classification of different liver lesions: comparison of Gd-EOB-DTPA-enhanced MRI versus multiphasic spiral CT in a clinical single centre investigation. *Eur J Radiol.* 2013;82:1860–1869.
11. Di Martino M, Marin D, Guerrisi A, et al. Intraindividual comparison of gadoxetate disodium-enhanced MR imaging and 64-section multidetector CT in the detection of hepatocellular carcinoma in patients with cirrhosis. *Radiology.* 2010;256:806–816.
12. Haradome H, Grazioli L, Tinti R, et al. Additional value of gadoxetic acid-DTPA-enhanced hepatobiliary phase MR imaging in the diagnosis of early-stage hepatocellular carcinoma: comparison with dynamic triple-phase multidetector CT imaging. *J Magn Reson Imaging.* 2011;34:69–78.
13. Liberati A, Altman DG, Tetzlaff J, et al. The PRISMA statement for reporting systematic reviews and meta-analyses of studies that evaluate health care interventions: explanation and elaboration. *Ann Intern Med.* 2009;151:W65–W94.
14. Whiting PF, Rutjes AW, Westwood ME, et al., QUADAS-2 Group. QUADAS-2: a revised tool for the quality assessment of diagnostic accuracy studies. *Ann Intern Med.* 2011;155:529–536.
15. Mahajan N, Polavaram L, Vankayala H, et al. Diagnostic accuracy of myocardial perfusion imaging and stress echocardiography for the diagnosis of left main and triple vessel coronary artery disease: a comparative meta-analysis. *Heart.* 2010;96:956–966.
16. Rosman AS, Korsten MA. Application of summary receiver operating characteristics (sROC) analysis to diagnostic clinical testing. *Adv Med Sci.* 2007;52:76–82.
17. Ooka Y, Kanai F, Okabe S, et al. Gadoxetic acid-enhanced MRI compared with CT during angiography in the diagnosis of hepatocellular carcinoma. *Magn Reson Imaging.* 2013;31:748–754.
18. Sano K, Ichikawa T, Motosugi U, et al. Imaging study of early hepatocellular carcinoma: usefulness of gadoxetic acid-enhanced MR imaging. *Radiology.* 2011;261:834–844.
19. Sun HY, Lee JM, Shin CI, et al. Gadoxetic acid-enhanced magnetic resonance imaging for differentiating small hepatocellular carcinomas (≤2 cm in diameter) from arterial enhancing pseudolesions: special emphasis on hepatobiliary phase imaging. *Invest Radiol.* 2010;45:96–103.
20. Kim SH, Kim SH, Lee J, et al. Gadoxetic acid-enhanced MRI versus triple-phase MDCT for the preoperative detection of hepatocellular carcinoma. *AJR Am J Roentgenol.* 2009;192:1675–1681.
21. Hamm B, Staks T, Mühler A, et al. Phase I clinical evaluation of Gd-EOB-DTPA as a hepatobiliary MR contrast agent: safety, pharmacokinetics, and MR imaging. *Radiology.* 1995;195:785–792.
22. Akai H, Kiryu S, Takao H, et al. Efficacy of double-arterial phase gadolinium ethoxybenzyl diethylenetriamine pentaacetic acid-enhanced liver magnetic resonance imaging compared with double-arterial phase multi-detector row helical computed tomography. *J Comput Assist Tomogr.* 2009;33:887–892.
23. Lee CH, Kim KA, Lee J, et al. Using low tube voltage (80 kVp) quadruple phase liver CT for the detection of hepatocellular carcinoma: two-year experience and comparison with Gd-EOB-DTPA enhanced liver MRI. *Eur J Radiol.* 2012;81:e605–e611.
24. Kim YK, Kim CS, Han YM, et al. Detection of hepatocellular carcinoma: gadoxetic acid-enhanced 3-dimensional magnetic resonance imaging versus multi-detector row computed tomography. *J Comput Assist Tomogr.* 2009;33:844–850.
25. Onishi H, Kim T, Imai Y, et al. Hypervascular hepatocellular carcinomas: detection with gadoxetate disodium-enhanced MR imaging and multiphasic multidetector CT. *Eur Radiol.* 2012;22:845–854.
26. Park MJ, Kim YK, Lee MH, et al. Validation of diagnostic criteria using gadoxetic acid-enhanced and diffusion-weighted MR imaging for small hepatocellular carcinoma (≤2.0 cm) in patients with hepatitis-induced liver cirrhosis. *Acta Radiol.* 2013;54:127–136.
27. Rhee H, Kim MJ, Park YN, et al. Gadoxetic acid-enhanced MRI findings of early hepatocellular carcinoma as defined by new histologic criteria. *J Magn Reson Imaging.* 2012;35:393–398.
28. Toyota N, Nakamura Y, Hieda M, et al. Diagnostic capability of gadoxetate disodium-enhanced liver MRI for diagnosis of hepatocellular carcinoma: comparison with multi-detector CT. *Hiroshima J Med Sci.* 2013;62:55–61.
29. Hwang J, Kim SH, Lee MW, et al. Small (≤2 cm) hepatocellular carcinoma in patients with chronic liver disease: comparison of gadoxetic acid-enhanced 3.0 T MRI and multiphasic 64-multirow detector CT. *Br J Radiol.* 2012;85:e314–e322.
30. Inoue T, Kudo M, Komuta M, et al. Assessment of Gd-EOB-DTPA-enhanced MRI for HCC and dysplastic nodules and comparison of detection sensitivity versus MDCT. *J Gastroenterol.* 2012;47:1036–1047.
31. Ichikawa T, Saito K, Yoshioka N, et al. Detection and characterization of focal liver lesions: a Japanese phase III, multicenter comparison between gadoxetic acid disodium-enhanced magnetic resonance imaging and contrast-enhanced computed tomography predominantly in patients with hepatocellular carcinoma and chronic liver disease. *Invest Radiol.* 2010;45:133–141.

32. Yoo SH, Choi JY, Jang JW, et al. Gd-EOB-DTPA-enhanced MRI is better than MDCT in decision making of curative treatment for hepatocellular carcinoma. *Ann Surg Oncol.* 2013;20:2893–2900.

33. Zech CJ, Korpraphong P, Huppertz A, et al., VALUE study group. Randomized multicentre trial of gadoxetic acid-enhanced MRI versus conventional MRI or CT in the staging of colorectal cancer liver metastases. *Br J Surg.* 2014;101:613–621.

34. Liu X, Zou L, Liu F, et al. Gadoxetic acid disodium-enhanced magnetic resonance imaging for the detection of hepatocellular carcinoma: a meta-analysis. *PLoS One.* 2013;8:e70896.

35. Chen L, Zhang J, Zhang L, et al. Meta-analysis of gadoxetic acid disodium (Gd-EOB-DTPA)-enhanced magnetic resonance imaging for the detection of liver metastases. *PLoS One.* 2012;7: e48681.

36. Kim YK, Kim CS, Han YM, et al. Detection of small hepatocellular carcinoma: intraindividual comparison of gadoxeticacid-enhanced MRI at 3.0 and 1.5 T. *Invest Radiol.* 2011;46:383–389.

37. Kim SH, Lee WJ, Lim HK, et al. SPIO-enhanced MRI findings of well-differentiated hepatocellular carcinomas: correlation with MDCT findings. *Korean J Radiol.* 2009;10:112–120.